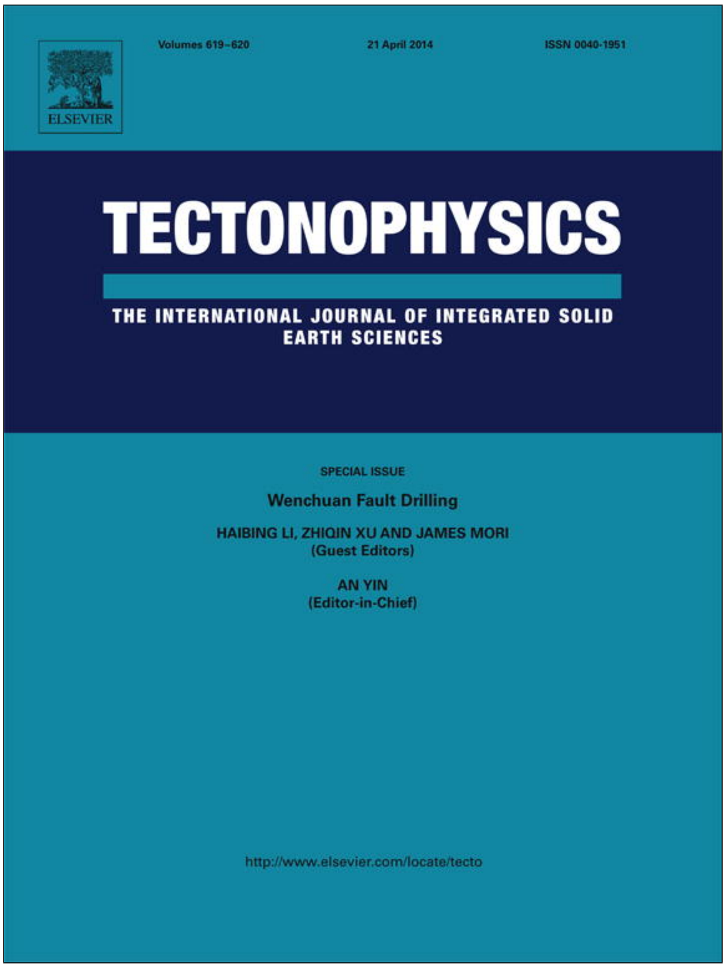
Volumes 619–620
21 April 2014
ISSN 0040-1951
ELSEVIER
TECTONOPHYSICS
THE INTERNATIONAL JOURNAL OF INTEGRATED SOLID EARTH SCIENCES
SPECIAL ISSUE
Wenchuan Fault Drilling
HAIBING LI, ZHIQIN XU AND JAMES MORI
(Guest Editors)
AN YIN
(Editor-in-Chief)
http://www.elsevier.com/locate/tecto

Tectonophysics 619–620 (2014) 29–35

Contents lists available at ScienceDirect

Tectonophysics

journal homepage: www.elsevier.com/locate/tecto

Coseismic thickness of principal slip zone from the Taiwan Chelungpu fault Drilling Project-A (TCDP-A) and correlated fracture energy

Li-Wei Kuo [a,*], Hsiu-Ching Hsiao [a], Sheng-Rong Song [a], Hwo-Shuenn Sheu [b], John Suppe [a]

[a] Department of Geosciences, National Taiwan University, Taiwan
[b] National Synchrotron Radiation Research Center, Taiwan

ARTICLE INFO

Article history:
Received 31 January 2013
Received in revised form 26 June 2013
Accepted 4 July 2013
Available online 11 July 2013

Keywords:
Principal slip zone
Chelungpu fault
TCDP
Synchrotron
Fracture energy
Pseudotachylyte

ABSTRACT

Direct observations of the physical structures of the seismogenic zones of active faults are rare, due to the difficulty in reaching the fault zone at depth. Current geological evidences, mostly from the surface, suggest that principal slip zone (PSZ) accommodated most shear displacement and was the place where physico-chemical processes occurred during an individual coseismic event and the thickness of PSZ is a few millimeter to tens of centimeter wide. However, the actual thickness of PSZ of a large earthquake, a key parameter of seismology in understanding energy dissipation and rupture processes, remains largely unknown. The Chelungpu fault that ruptured during the 1999 Mw 7.6 Chi-Chi earthquake (Taiwan) was drilled to a depth of 2003 m providing a unique opportunity to sample an active fault that slipped in a recent large earthquake. The PSZ, corresponding to the 1999 Chi-Chi earthquake, was well characterized within cores at a borehole depth of 1111 m from the Taiwan Chelungpu fault Drilling Project-A (TCDP-A). Here we determine the interval of clay anomaly that resulted from frictional melting/thermal decomposition process by state-of-art in-situ synchrotron XRD analysis providing very high spatial resolution for mineralogy. Combined with the interval of the presence of vesicles from microstructural observation, the thickness of Chi-Chi PSZ is estimated to be 1 mm. Thus, the correlated contribution of surface fracture energy to earthquake breakdown work, at least in this locality, is quantified to be 1.9%. The huge remaining part of the breakdown work seems to be turned into heat associated with fault dynamic processes during the 1999 Chi-Chi earthquake.

1. Introduction

A brittle fault zone commonly shows three major internal components: fault core, damage zone, and host rock (Chester et al., 1993). The host rock or protolith remains basically undamaged during coseismic events. The damage zone is characterized by an increased density of subsidiary faults, fractures, veins, foliation, and folding relative to the host rock. The fault core, such as fault gouge, is typically characterized by geochemically altered and comminuted rocks produced during coseismic events and/or aseismic periods. Principal slip zone (PSZ: Sibson, 2003) within the fault core accommodated most shear displacement and/or high strain and was the place where physico-chemical processes were driven during an individual coseismic event. To aim at the fault zone geology (e.g., fault behavior such as weakening and involved mechanism, energy budget such as energy dissipation), a critical and challenging prospect, the identification of PSZ and its associated structures and reactions in an individual fault, is arising (Boullier, 2011).

Several scientific continental fault-zone drilling projects were conducted and these include the Nojima fault project following the 1995 Kobe earthquake in Japan (Boullier et al., 2001); the Taiwan Chelungpu fault Drilling Project (TCDP) following the 1999 Chi-Chi earthquake in Taiwan (Ma et al., 2006); the San Andreas Fault Observatory at Depth (SAFOD) in the U.S.A., (Zoback et al., 2010); and the Wenchuan earthquake Fault Scientific Drilling (WFSD) following the 2008 Wenchuan earthquake in China, (Li et al., 2013). The main goals of these drilling projects are to measure in-situ stress, strain, pore pressure, and other physical properties within active fault zones (e.g., porosity and permeability) (e.g., Zoback et al., 2010). Whereas, weathering (and exhumation) might erase and/or transform the signature, recorded in the fault rocks, of the physico-chemical process (e.g., melting, dehydration, etc.) occurring at depth during seismic slips (e.g., Kuo et al., 2012). To diminish the effects resulted from postseismic alteration on fault rocks, these continental fault-zone drilling projects could also provide fresh fault rocks to be directly investigated the physico-chemical processes within active fault zones (PSZ) during coseismic events. In this study, the recognition of PSZ corresponding to the 1999 Chi-Chi earthquake in Taiwan was based on the current literature from the TCDP and the details will be described later.

On 21st September 1999 the N–S-trending Chelungpu thrust fault ruptured in a Mw 7.6 earthquake near the town of Chi-Chi, producing 90-km long surface ruptures (Fig. 1a) (Lee et al., 2001). TCDP was initiated around six years after the mainshock with the intention of

* Corresponding author at: No. 1, Sec. 4, Roosevelt Road, Taipei 10617, Taiwan. Fax: +886 2 23636095.
E-mail address: liweikuo@ntu.edu.tw (L.-W. Kuo).

0040-1951/$ – see front matter
http://dx.doi.org/10.1016/j.tecto.2013.07.006

penetrating the Chelungpu fault at depth (Fig. 1b). The drill site of TCDP is 2-km east of the recently surface ruptured slip zone in the northern portion of the Chelungpu fault (Ma et al., 2006). The spatial slip distribution for the earthquake was well constrained from close strong motion and GPS data and showed a slip of 8.3 m on the fault near the drill site (Ji et al., 2003; Ma et al., 2001; Yue et al., 2005). TCDP was carried out a continuous coring for depths of 500 m to 2003 m, and 950 m to 1300 m for hole-A and hole-B, respectively. The fault core identified from the continuous core images was located at the depth of 1111 m of hole-A and 1137 m of hole-B, respectively (Fig. 1c for hole-A). The black gouge within the fault core, containing a band of highly intense grain-size reduction, was identified as the Chi-Chi PSZ (Ma et al., 2006).

The distinguishing characteristics were discovered within the PSZ: grain size distribution (Ma et al., 2006), microstructures (Boullier et al., 2009), clay–clast aggregates (CCAs) (Boutareaud et al., 2008, 2010), magnetic anomaly (Chou et al., 2012a, b; Hirono et al., 2006a; Mishima et al., 2006, 2009), inorganic carbon content (Hirono et al., 2006b), major and trace elements (Ishikawa et al., 2008), and clay anomaly (Hirono et al., 2008; Kuo et al., 2009, 2011). On the basis of current literature we presumably suggest that the formation of PSZ was due to the 1999 Chi-Chi earthquake.

The thickness of Chi-Chi PSZ from the aspect of microstructures was estimated to obtain the surface fracture energy and associated seismic efficiency (Ma et al., 2006). In this study we re-examine the thickness of PSZ from the aspect of mineralogy through characterizing the interval of clay anomaly with the in-situ synchrotron X-ray analysis. Furthermore, we also integrate our results with microstructures and the literature data from Ma et al. (2006) to obtain the correlated contribution of the fracture energy to the earthquake breakdown work.

2. Sample description and analytical methods

2.1. Petrographic thin section of Chi-Chi PSZ

The fault core of the Chelungpu fault was obtained from 1110.37 m to 1111.45 m depth in TCDP-A (Fig. 1c) and was made into sixteen

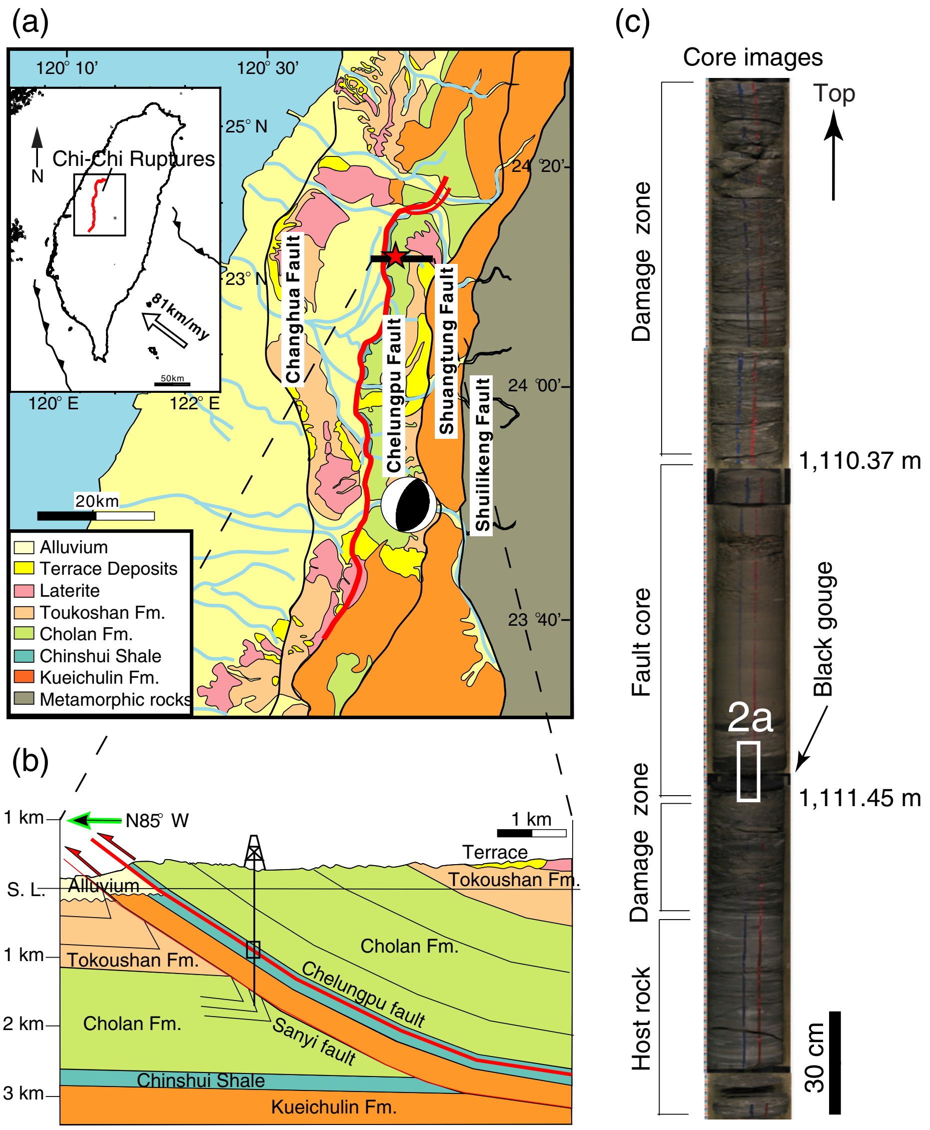

Fig. 1. Geological setting of the 1999 Mw 7.6 Chi-Chi earthquake and location of the TCDP-A drilling site. (a) Location of the TCDP-A drilling site and the 90-km-long surface ruptures associated with the Mw 7.6 earthquake at the central part of western Taiwan. The TCDP site is indicated by a red star. The focal mechanism of the Chi-Chi main shock is located at the hypocenter of the Chi-Chi earthquake. The insert box is the tectonic setting of Taiwan. (b) An E–W cross section of the TCDP-A showing the Chelungpu fault zone and surrounding formations encountered in the borehole (after Hung et al., 2007). The rectangle displaying the principal slip zone active during the 1999 mainshock was identified in the borehole at 1111.29 m depth and the images of fault core samples of the TCDP-A was enlarged in the right panel as (c). (C) The image exhibiting major portions of the Chelungpu-fault along the borehole of TCDP.

petrographic thin sections. The thin section of black gouge (2.1 × 3.5 cm) enclosing Chi-Chi PSZ was utilized (Fig. 2a) for microstructural observation and mineralogical investigation. The direction of slip shown on the thin section approximately ranged from 20 to 30° dipping leftward (Fig. 2a, b). The central part of the petrographic thin section was observed with the direction of parallel to the long sides and perpendicular to the thin section as shown in Fig. 2b.

2.2. Field emission scanning electron microscope with energy dispersive spectrometer (FESEM/EDX)

To observe the characteristics and semi-quantify the chemical composition of PSZ, we utilized FESEM/EDX quantitative analysis with a FEI QUANTA 200F scanning electron microscope coupled to an energy dispersive spectrometer at 10 KV with the standardized processes at the National Taiwan University (NTU).

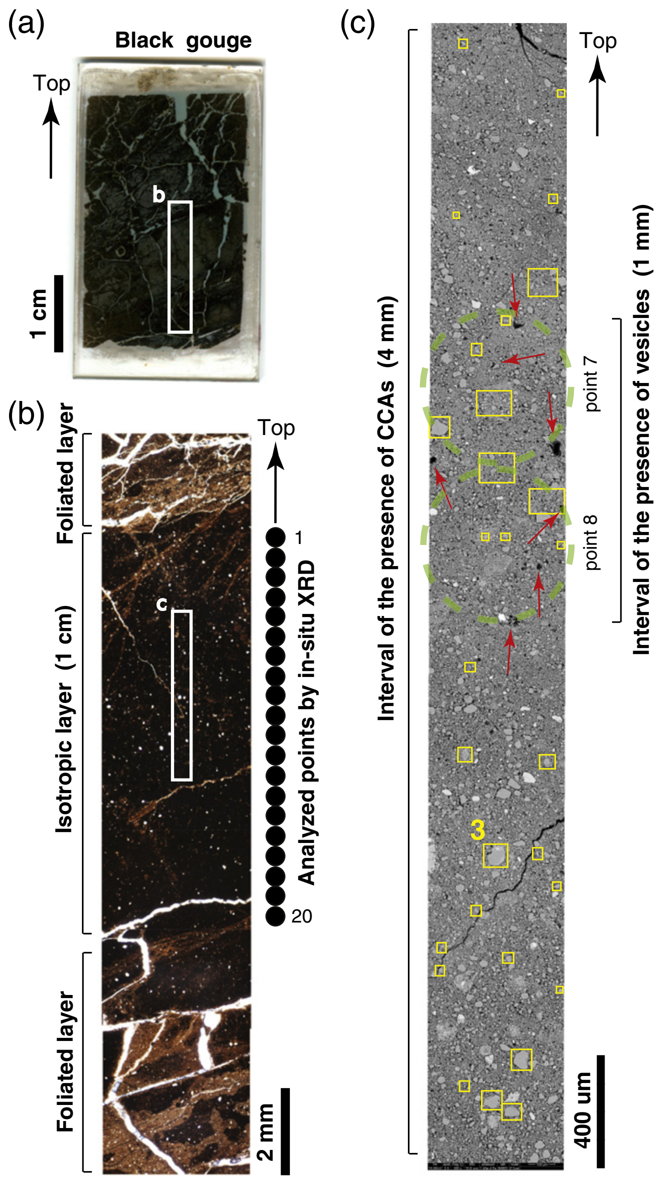

Fig. 2. Microstructural observation of black gouge hosting the Chi-Chi PSZ. (a) The scan of the thin section of black gouge indicating the fracturing zone and the isotropic layer. (b) Microstructures in the isotropic layer showing the matrix-support clasts which are quartz fragments and ultrafine grained clays defined as the isotropic layer by Boullier et al. (2009). Twenty analyzed points by in-situ synchrotron XRD were shown in the right side of the image. (c) Backscattered electron SEM images of the isotropic layer contains large quartz clasts, very fine grains of clays, vesicles indicated by red arrows, and CCAs marked with yellow rectangular boxes. One representative CCA was shown in Fig. 3.

2.3. In-situ synchrotron X-ray diffraction analysis

The in-situ X-ray diffraction was performed at the beamline BL01C2 of National Synchrotron Radiation Research Center (NSRRC) Taiwan. The synchrotron X-ray radiation was generated from the superconducting wavelength shifted magnet of 5.0 T with ring energy of 1.5 GeV typical ring current of 200 to 120 mA. The X-ray wavelength was 0.5166 Å which delivered by a double crystal monochromator with two Si(111) crystals. The PSZ was continuously analyzed with the beam size of 500 μm diameter during the X-ray measurement. Two dimensional powder X-ray diffraction patterns were recorded by using Mar345 imaging plate detector with the pixel size of 100 μm and the typical exposure time of 60 s. The one dimensional XRD profile was converted using the FIT2D program of a cake type integration.

3. Results

3.1. Microstructural observation of black gouge

A 1-cm thick layer characterized by an ultrafine grain matrix with suspended clasts was found in the black gouge (Fig. 2b). The 1-cm thick gouge layer did not contain any fracture, cleavage, vein, banding, or shearing structure and was defined as the isotropic layer (following by Boullier et al., 2009). The isotropic layer was surrounded by foliated layers which contain deformed veins, oriented clay-rich layers, fragments of old gouges and quartz, and cracks.

The clastic cores mantled by concentric fine-grained aggregated materials called clay–clast aggregates (CCAs) (Boutareaud et al., 2008) were found in 4-mm thick layer within the isotropic layer (Fig. 2c). The inner cores (central clasts hereafter) of the CCAs were fragments of quartz and feldspar, and the diameter of the central clasts was between 1 and 130 μm. The CCAs were marked with yellow rectangular boxes in Fig. 2c and were not found in the surrounding black gouges or elsewhere in the fault zone. FESEM/EDX element mapping conducted on a typical monomineralic CCAs displays a higher relative atomic density of Al, Na, K, Fe and Mg in the cortex which highlights clays concentrically coating the central clast which the atomic density is dominant in Si (Fig. 3). In addition, the vesicles presumably resulted from thermal decomposition/dehydroxylation processes (Kuo et al., 2009, 2011) were indicated by red arrows (Fig. 2c). The presence of vesicles was estimated as 1-mm thick within the isotropic layer.

3.2. Characteristics of mineralogy in PSZ

Twenty analyses of the in-situ synchrotron XRD, from top to bottom of the isotropic layer on thin section, were conducted to obtain the mineral assemblage (Fig. 2b). The average value of twenty XRD curves was plotted as the black line and the mineral phases of the isotropic layer were identified as quartz, feldspar, calcite, illite and very few smectite (Fig. 4a). The bump from 15 to 40 of two thetas in all synchrotron analyses resulted from the signal of thin section made by glass. The tiny signal of smectite was captured and was enlarged in Fig. 4b. Two degrees of relatively high abundances of smectite were observed and were drawn in red lines and blue lines, respectively. The in-situ XRD data shows that the relatively high abundance of smectite (the point 7 and the point 8) was located in the interval of the presence of vesicles (Fig. 2c, see also Kuo et al., 2009).

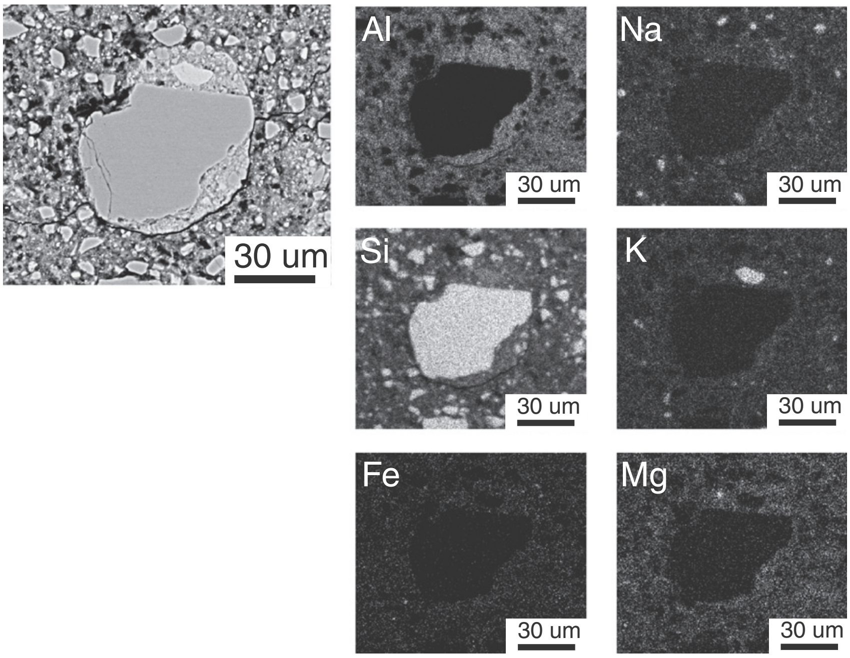

Fig. 3. EDX–SEM element composition mapping of a typical CCA in the isotropic layer. Only Al, Na, K, Fe and Mg elements show a strong signal for the cortex of CCAs.

4. Discussion

4.1. Thickness of Chi-Chi PSZ

The Chi-Chi PSZ accommodated a coseismic displacement of 8.3 m with a maximum slip velocity of 3 m/s (Ma et al., 2006), and the evidences of thermal perturbations (Chou et al., 2012a, b; Hirono et al., 2006b, 2008; Ishikawa et al., 2008; Kuo et al., 2009, 2011; Mishima et al., 2006, 2009) and fluid infiltrations (Chou et al., 2012a, b; Ishikawa et al., 2008) within the PSZ were obtained from borehole core samples. It suggests that several physico-chemical processes were triggered during past coseismic events and one speculated reaction was proposed as thermal decomposition/dehydroxylation of clay minerals in TCDP-A (Kuo et al., 2009). The relative weight percentage of individual clay mineral shows that the content of smectite in core samples was rare to nonexistent from 500 to 2003 m depth, instead of the one of PSZ (Kuo et al., 2011). The abundance of smectite (80%) within the PSZ was proposed as the product resulted from the alteration of amorphous materials. Amorphous materials can be produced by melting during frictional seismic sliding (0.1–3 m/s) (e.g., Di Toro et al., 2006), and also at subseismic slip rates ($\ll$0.1 m/s) (Pec et al., 2012; Yund et al., 1990). In TCDP case, the stresses, ambient temperature and displacement at TCDP borehole depth are of the order of tens of MPa, less than 50 °C, and 6–9 m, respectively (Ji et al., 2003; Tanaka et al., 2007). It seems that amorphous materials within the PSZ were neither at high stresses (up to 1.5 GPa) and large ambient temperature (300 to 500 °C) suggested by Pec et al. (2012), nor with the short displacement (less than 40 cm) conducted by Yund et al. (1990). The amorphous materials in the PSZ that were presumably the product of solidification of melts (pseudotachylyte) resulted from frictional seismic slips. The glass–smectite reaction was well documented in many natural environments and laboratories (e.g., Bauluz et al., 2004), and the experimental evidence suggested that the advance of glass–smectite reaction only took 3 days at 90 °C with 1–10 M NaOH solution (Tomita et al., 1993). On the basis of the observation of thermal perturbations and fluid infiltrations in the Chi-Chi slip zone (Chou et al., 2012a, b; Ishikawa et al., 2008; Mishima et al., 2006), it is reasonable to conclude that the transformation of smectite from glass occurred in less than a few days to years post the Chi-Chi earthquake. In addition, the similar transformation of glass–smectite within the active fault zone of the Nojima fault was determined by TEM analysis and the presence of smectite also inferred the alteration of pseudotachylyte (Janssen et al., 2013). In summary, the presence of smectite within PSZ was derived from the alteration of pseudotachylyte and/or amorphous materials resulted from frictional heating during the 1999 Chi-Chi earthquake (Kuo et al., 2009). The thickness of smectite-rich layer considered as the thickness of the PSZ was estimated as 2 cm due to the limitation of 2-cm interval of sampling for XRD powder analysis (Kuo et al., 2009).

On the basis of the characteristics of clays within PSZ, high spatial resolution synchrotron XRD analysis was conducted to determine the interval of smectite-rich layer. Although the traditional identification of swelling clays following the process of air-drying and ethylene-glycol solvation was not performed in this study, the distinct wide peak from 4 to 6 of two thetas (Fig. 4b) presumably resulted from new formed smectite suggested by Kuo et al. (2009). The relatively high abundance of smectite within the isotropic layer was detected in point 7 and point 8, and relatively moderate abundance of smectite was detected in point 9 and point 10 (Fig. 4b). Combined with the occurrence of vesicles that likely resulted from frictional heat (Fig. 2c) (Kuo et al., 2011), the interval of the thermal perturbation where the process of thermal decomposition/dehydroxylation occurred was estimated as 1 mm.

The formation of CCAs in fault gouges caused by seismic faulting is still a debate (Han and Hirose, 2012). Han and Hirose (2012) systematically conducted rock deformation experiments at a wide range of slip rates and demonstrated that the presence of CCAs was not necessarily produced at seismic rates. As we mentioned above, amorphous materials within the PSZ were generated by frictional seismic slips during Chi-Chi event (Kuo et al., 2009). The CCAs were only observed within the isotropic layer which were accompanied by the PSZ (Fig. 2c). It suggests that the CCAs were plausibly produced at seismic rates, at least in this locality. In addition, considering the infiltrations of coseismic fluid mentioned above, the occurrence of CCAs appears to be a possible indicator for thermal pressurization and/or gouge fluidization in TCDP case as suggested by Boutareaud et al. (2010). The interval of the presence of CCAs was estimated as 4 mm (Fig. 2c) which might illustrate the affected area of the mechanism of thermal pressurization.

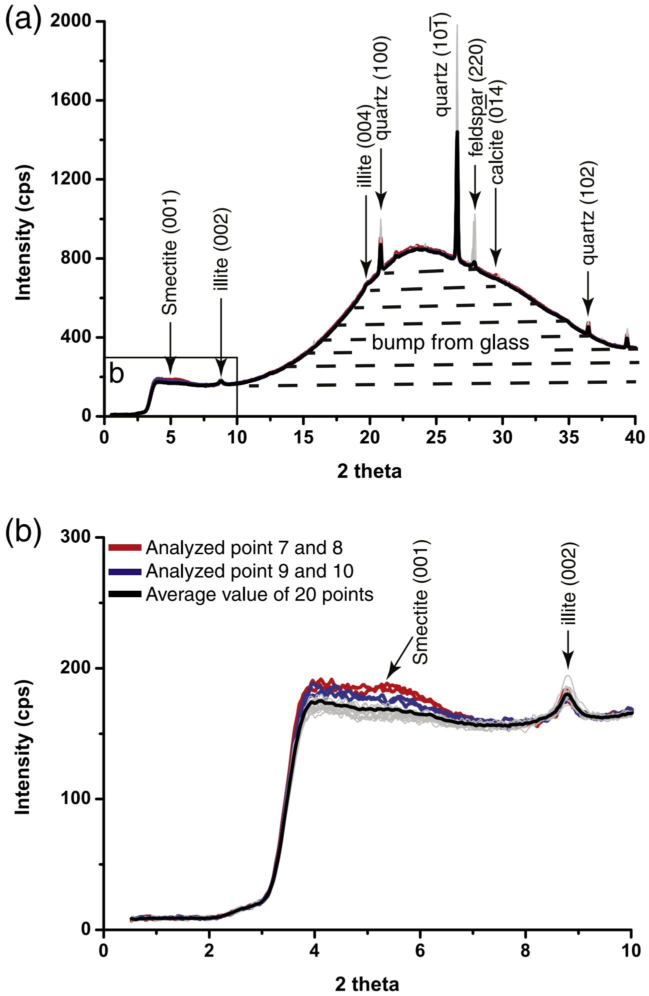

Fig. 4. (a) All apparent peaks are identified by the in-situ synchrotron XRD analyses and signed with mineral names. The bump caused by the peak of glass was drawn with dashed lines. The insert box is the signal of smectite and was enlarged in (b). (b) All results were drawn in light gray lines, and the average value of all experiments was drawn in black lines except relatively high abundance of smectite. The highest abundance of smectite was drawn in red lines and the moderate one was drawn in blue lines.

The thickness of PSZ from the aspect of microstructural observation was obtained as (1) 2 cm identified from the fault core of TCDP (Boullier et al., 2009; Ma et al., 2006), (2) 50–300 μm of fault cores from surface outcrops (Heermance et al., 2003), and (3) 7 mm of fault gouge at 330 m depth from shallow hole (Tanaka et al., 2002). The variation of the thickness of PSZ might be due to the heterogeneity of the fault at different depths (Gratier et al., 2003) and this issue is not probed in this study. In summary, 1-mm thickness was obtained from the interval of thermal decomposition/dehydroxylation of clay minerals and 4-mm thickness was measured from the interval of the presence of CCAs within the isotropic layer. Here we utilize 1 mm as the thickness of Chi-Chi PSZ followed by the definition of PSZ which accommodated most shear displacement and/or high strain followed with high frictional heat generated.

4.2. Surface fracture energy of PSZ and contribution of the breakdown work

The breakdown work, considered as an equivalent to seismic fracture energy, is the energy spent for rupture to advance during earthquakes (Tinti et al., 2005). The breakdown work is composed of surface fracture energy and plastic deformation of grains associated with the creation of small grains within the slipping zones, and frictional heat driving physico-chemical processes along the fault slip surface. The breakdown work could be obtained by calculating the integral of the shear traction versus slip, from zero slip to the point that the traction drops to a minimum (Tinti et al., 2005):

$$W_b = \int_0^{t_b} (\tau(t) - \tau_{min}) \bullet v(t) dt \tag{1}$$

where $v(t)$ is the slip velocity, $\tau(t)$ is the shear traction, and t_b is the time at which minimum traction τ_{min} is reached. In TCDP case, a grid size (fault block) of 0.95 km and a time interval of 0.054 s, based on the kinematic results of the temporal–spatial slip distribution (Ji et al., 2003), were used to calculate the breakdown work. The shear traction (stress–slip curve) was obtained by combining the stress-time history and slip-time history from kinematic inversion. The integral of Eq. (1) gives a value of the breakdown work of 11.6 MJ m^{-2} for a small patch of the subfault 1 km beneath the drill site (Ma et al., 2006). Several assumptions were made for the calculation as following: 1) the breakdown work was homogeneously distributed beneath the drill site over the subfault, 2) fault core thickness, fault geometry, and grain size distribution did not vary in the subfault. Ben-Zion and Sammis (2003) determined how different aspects of a fault zone may be alternatively described in different frameworks, and the clarification of the assumption, either from field geology side or from the laboratory side, still remains challenging (Niemeijer et al., 2012). The value of breakdown work obtained in this study might be risky to stand for the 1999 Chi-Chi earthquake, but at least it is convincible at this locality.

The particle surface area (S_{msz}) of the major slip zone (MSZ) of TCDP-A was obtained from the microstructural observation and the value of S_{msz} was estimated of 6.46×10^5 m^2 per meter squared area (Ma et al., 2006). The mineral composition of MSZ which was composed of 70% of quartz, 5% feldspar, and 25% clays gives a specific fracture energy G_c of about 1 J m^{-2} (McGarr et al., 1979; Scholz, 2002). A corrected parameter for grain roughness λ of 0.66 was utilized (Wilson et al., 2005). Thus, the total surface fracture energy (G_{msz}) of the 2-cm MSZ of TCDP-A was obtained by:

$$G_{msz} = S_{msz} \lambda G_c. \tag{2}$$

Ma et al. (2006) provided a value of 4.3 MJ per meter squared area for the total surface fracture energy from Eq. (2). Since the fault materials of the 2-cm MSZ defined by Ma et al. (2006) is consistent with the one of the isotropic layer in this study, the total surface fracture energy can be proportionally utilized for the 1-cm isotropic layer and the value of total surface fracture energy would be 2.15 MJ per meter squared area.

On the basis of the determination of the PSZ, 1-mm thick gouge was formed for the specific event of the 1999 Chi-Chi earthquake. The 1-cm thick isotropic layer seems to be the accumulation of PSZ since it was not produced by only one coseismic event. The maximum number of repeated earthquakes in the 1-cm isotropic layer is roughly estimated as 10 if we assume similar displacement of repeating earthquakes in the isotropic layer. Several assumptions were made as following: 1) all the earthquakes accommodated similar slips, 2) each earthquake should occur in the slipping zones next to the one where the previous earthquake ruptured and none of the slipping zones was exploited twice, and 3) there was no postseismic slip within the isotropic layer. We could not strictly constrain the coseismic slip of each individual earthquake, but the trenching in the southern part of the Chelungpu fault suggests that the magnitude of coseismic events similar to the one of Chi-Chi earthquake took place for several times (Chen et al., 2004). It implies that similar slips along the Chelungpu fault were produced in the coseismic events. We could not promise that coseismic slips always occurred within the isotropic layer, but smectite is one of the weakest known minerals and it may have controlled dynamic fault strength within the PSZ during coseismic events (Moore and Lockner, 2004). It seems that the location of the PSZ or close to this zone could be the candidate for the following seismic slips and then thickens the isotropic layer. In addition, postseismic slips were determined as 200–300 mm for 10 years in the northern segment of the Chelungpu fault (Rousset et al., 2012), but the short postseismic slips might not generate efficient energy to pulverize grains and/or rocks and may not make great influence on the calculation of the surface fracture energy. Thus, the minimum surface fracture energy associated to a single large earthquake on average (e.g., 1999 Chi-Chi earthquake) was 0.22 MJ per meter squared area.

Given the breakdown work of 11.6 MJ m^{-2}, the correlated contribution of the surface fracture energy corresponding to the 1999 Chi-Chi earthquake is estimated to be 1.9%. We consider the estimate to be the minimum for the assumption that the surface fracture energy generated within the Chelungpu fault zone 1 km beneath the drill site was negligible during the earthquake. The similar estimates which the surface fracture energy 0.10–0.85 MJ m^{-2} were compared to the work absorbed in frictional heating were obtained for pseudotachylyte-bearing faults and it also suggests that the almost total mechanical work was dissipated as frictional heat during coseismic events (Di Toro et al., 2005; Pittarello et al., 2008). It is notable that in the case of seismic ruptures propagating at shallow depths (<2 km) the amount of surface energy could be larger (e.g., Dor et al., 2006; Reches and Dewers, 2005). Since the surface fracture energy is much less in this study, it suggests that the huge remaining part of the breakdown work would be turned into chemical work (mineral transformations, fluid–rock interaction) (Chou et al., 2012a,b; Hirono et al., 2008; Kuo et al., 2009), and mechanic work which was associated with several processes suggested to result in coseismic fault lubrication such as thermal pressurization (Boullier et al., 2009; Hirono and Tanikawa, 2011), elastohydrodynamic lubrication (Brodsky and Kanamori, 2001), and frictional melting lubrication (Di Toro et al., 2006).

5. Conclusion

The interval of clay anomaly corresponding to the 1999 Chi-Chi earthquake has been determined with high spatial resolution in-situ synchrotron XRD analysis. Combined with the microstructural observation within the isotropic layer, the interval of clay anomaly was considered as the thickness of the Chi-Chi PSZ and was estimated to be 1 mm. The surface fracture energy of 0.22 MJ per meter squared area was obtained with the identification of the 1-mm PSZ. Following the earthquake breakdown work given by Ma et al. (2006), the contribution of the surface fracture energy to the earthquake breakdown work is estimated to be 1.9%. The extremely low contribution of fracturing in TCDP case suggests that most breakdown work was turned into heat associated with physico-chemical processes to result in fault lubrication during the 1999 Chi-Chi earthquake.

Acknowledgments

We would like to thank the editor and two anonymous reviewers for their criticisms and very constructive comments, which helped to improve the manuscript. We thank the working group of TCDP, including the drilling company Fang-Yu and Wan-Da, the on-site assistants and participating students from NTU and NCU. The research was supported by the National Science Council, Republic of China, under Grants of NSC 101-2116-M-002-006, and 101-2116-M-002-031, and the Wenchuan Earthquake Fault Scientific Drilling of the National Science and Technology Planning Project.

References

Bauluz, B., Peacor, D.R., Hollis, C.J., 2004. TEM study of meteorite impact glass at New Zealand Cretaceous–Tertiary sites: evidence for multiple impacts or differentiation during global circulation? Earth and Planetary Science Letters 219, 209–219.
Ben-Zion, Y., Sammis, C.G., 2003. Characterization of fault zones. Pure and Applied Geophysics 160, 677–715.
Boullier, A.-M., 2011. Fault-zone geology: lessons from drilling through the Nojima and Chelungpu fault. Geological Society of London, Special Publications 359, 17–37.
Boullier, A.-M., Ohtani, T., Fujimoto, K., Ito, H., Dubois, M., 2001. Fluid inclusions in pseudotachylytes from the Nojima Fault, Japan. Journal of Geophysical Research 106 (B10), 21965–21977.
Boullier, A.-M., Yeh, E.C., Boutareaud, S., Song, S.R., Tsai, C.H., 2009. Micro-scale anatomy of the 1999 Chi-Chi earthquake fault zone. Geochemistry, Geophysics, Geosystems 10 (3), Q03016.
Boutareaud, S., Calugaru, D.-G., Han, R., Fabbri, O., Mizoguchi, K., Tsutsumi, A., Shimamoto, T., 2008. Clay–clast aggregates: a new textural evidence for seismic fault sliding? Geophysical Research Letters 35 (5), L05302.
Boutareaud, S., Boullier, A.M., Andréani, M., Calugaru, D.G., Beck, P., Song, S.R., Shimamoto, T., 2010. Clay clast aggregates in gouges: new textural evidence for seismic faulting. Journal of Geophysical Research 115, B02408. http://dx.doi.org/10.1029/2008jb006254.
Brodsky, E.E., Kanamori, H., 2001. Elastohydrodynamic lubrication of faults. Journal of Geophysical Research 106, 16357–16374.
Chen, W.S., Lee, K.J., Lee, L.S., Ponti, D.J., Prentice, C., Chen, Y.G., Chang, H.C., Lee, Y.H., 2004. Paleoseismology of the Chelungpu fault during the past 1900 years. Quaternary International 115–116, 167–176.
Chester, F.M., Evans, J.P., Biegel, R.L., 1993. Internal structure and weakening mechanisms of the San Andreas Fault. Journal of Geophysical Research 98, 771–786.
Chou, Y.M., Song, S.R., Aubourg, C., Lee, T.Q., Boullier, A.-M., Song, Y.F., Yeh, E.C., Kuo, L.W., Wang, C.Y., 2012a. An earthquake slip zone is a magnetic recorder. Geology. http://dx.doi.org/10.1130/G32864.1.
Chou, Y.M., Song, S.R., Aubourg, C., Song, Y.F., Boullier, A.M., Lee, T.Q., Evans, M., 2012b. Pyrite alteration and neoformed magnetic minerals in the fault zone of the Chi-Chi earthquake (Mw 7.6, 1999): evidence for frictional heating and co-seismic fluids. Geochemistry, Geophysics, Geosystems 13 (8), Q08002. http://dx.doi.org/10.1029/2012GC004120.
Di Toro, G., Pennacchioni, G., Teza, G., 2005. Can pseudotachylyte be used to infer earthquake source parameter? An example of limitations in the study of exhumed faults. Tectonophysics 402, 3–20.
Di Toro, G., Hirose, T., Nielsen, S., Pennacchioni, G., Shimamoto, T., 2006. Natural and experimental evidence of melt lubrication of faults during earthquakes. Science 31, 647–649.
Dor, O., Ben-Zion, Y., Rockwell, T.K., Brune, J., 2006. Pulverized rocks in the Mojave section of the San Andreas fault zone. Earth and Planetary Science Letters 245, 642–654. http://dx.doi.org/10.1016/j.epsl.2006.03.034.
Gratier, J.-P., Favreau, P., Renard, F., 2003. Modeling fluid transfer along California faults when integrating pressure solution crack sealing and compaction process. Journal of Geophysical Research 108. http://dx.doi.org/10.1029/2001JB000380.
Han, R., Hirose, T., 2012. Clay–clast aggregates in fault gouge: an unequivocal indicator of seismic faulting at shallow depths? Journal of Structural Geology 43, 92–99.
Heermance, R.V., Shipton, Z.K., Evans, J.P., 2003. Fault structure control on fault slip and ground motion during the 1999 rupture of the Chelungpu fault, Taiwan. Bulletin of Seismological Society of America 93, 1034–1050.
Hirono, T., Tanikawa, W., 2011. Implications of the thermal properties and kinetic parameters of dehydroxylation of mica minerals for fault weakening, frictional heating, and earthquake energetics. Earth, Planets, and Space Letters 307, 161–172.
Hirono, T., Lin, W., Yeh, E.C., Soh, W., Hashimoto, Y., Sone, H., Matsubayashi, O., Aoike, K., Ito, H., Kinoshita, M., Murayama, M., Song, S.R., Ma, K.F., Hung, J.H., Wang, C.Y., Tsai, Y.B., 2006a. High magnetic susceptibility of fault gouge within Taiwan Chelungpu fault: nondestructive continuous measurements of physical and chemical properties in fault rocks recovered from Hole B, TCDP. Geophysical Research Letters 33, L15303. http://dx.doi.org/10.1029/2006GL026133.
Hirono, T., Ikehara, M., Otsuki, K., Mishima, T., Sakaguchi, M., Soh, W., Omori, M., Lin, W., Yeh, E.C., Tanikawa, W., Wang, C.Y., 2006b. Evidence of frictional melting within disk-shaped black materials discovered from the Taiwan Chelungpu fault system. Geophysical Research Letters 33, L19311. http://dx.doi.org/10.1029/2006GL027329.
Hirono, T., Fujimoto, K., Yokoyama, T., Hamada, Y., Tanikawa, W., Tadai, O., Mishima, T., Tanimizu, M., Lin, W., Soh, W., Song, S.R., 2008. Clay mineral reactions caused by frictional heating during an earthquake: an example from the Taiwan Chelungpu fault. Geophysical Research Letters 35, L16303. http://dx.doi.org/10.1029/2008GL034476.
Hung, J.H., Wu, Y.H., Yeh, E.C., Wang, J.C., 2007. Subsurface structure, physical properties, and fault zone characteristics in the scientific drill holes of Taiwan Chelungpu-Fault Drilling Project. Terrestrial Atmospheric and Oceanic Science 18, 271–293.
Ishikawa, T., Tanimizu, M., Nagaishi, K., Matsuoka, J., Tadai, O., Sakaguchi, M., Hirono, T., Mishima, T., Tanikawa, W., Lin, W., Kikuta, H., Soh, W., Song, S.R., 2008. Coseismic fluid–rock interactions at high temperatures in the Chelungpu fault. Nature Geosciences 1. http://dx.doi.org/10.1038/ngeo308.
Janssen, C., Wirth, R., Lin, A., Dresen, G., 2013. TEM microstructural analysis in a fault gouge sample of the Nojima fault zone, Japan. Tectonophysics 583, 101–104. http://dx.doi.org/10.1016/j.tecto.2012.10.020.
Ji, C., Helmberger, D.V., Wald, D.J., Ma, K.F., 2003. Slip history and dynamic implication of the 1999 Chi-Chi, Taiwan, earthquake. Journal of Geophysical Research 108 (B9), 2412. http://dx.doi.org/10.1029/2002JB001764.
Kuo, L.W., Song, S.R., Yeh, E.C., Chen, H.F., 2009. Clay mineral anomalies in the fault zone of Chelungpu Fault, Taiwan, and its implication. Geophysical Research Letters 36, L18306. http://dx.doi.org/10.1029/2009GL039269.
Kuo, L.W., Song, S.R., Huang, L., Yeh, E.C., Chen, H.F., 2011. Temperature estimates of coseismic heating in clay-rich fault gouges, the Chelungpu fault zone, Taiwan. Tectonophysics 502, 315–327.
Kuo, L.W., Song, S.R., Yeh, E.C., Chen, H.F., Si, J., 2012. Clay mineralogy and geochemistry investigations in the host rock of the Chelungpu fault, Taiwan: implication for faulting mechanism. Journal of Asian Earth Sciences 59, 208–218.

Lee, J.C., Chen, Y.G., Sieh, K., Mueller, K., Chen, W.S., Chu, H.T., Chan, Y.C., Rubin, C., Yates, R., 2001. A vertical exposure of the 1999 surface rupture of the Chelungpu fault at Wufeng, western Taiwan: structural and paleoseismic implications for an active thrust fault. Seismological Society of America 91 (5), 914–929.

Li, H.B., Wang, H., Xu, Z.Q., Si, J.L., Pei, J.L., Li, T.F., Yao, H., Song, S.R., Kuo, L.W., Sun, Z.M., Chevalier, M.L., Liu, D.L., 2013. Characteristics of the fault-related rocks, fault zones and the principal slip zone in the Wenchuan earthquake Fault Scientific Drilling project Hole-1 (WFSD-1). Tectonophysics 584, 23–42.

Ma, K.F., Mori, J., Lee, S.J., Yu, S.B., 2001. Spatial and temporal distribution of slip for the 1999 Chi-Chi, Taiwan, earthquake. Bulletin of the Seismological Society of America 91, 1069–1087.

Ma, K.F., Tanaka, H., Song, S.R., Wang, C.Y., Hung, J.H., Tsai, Y.B., Mori, J., Song, Y.F., Yeh, E.C., Soh, W., Sone, H., Kuo, L.W., Wu, H.Y., 2006. Slip zone and energetics of a large earthquake from the Taiwan Chelungpu-fault Drilling Project. Nature 444, 473–476.

McGarr, A., Spottiswoode, S.M., Gay, N., 1979. Observations relevant to seismic driving stress, stress drop, and efficiency. Journal of Geophysical Research 84, 2251–2261.

Mishima, T., Hirono, T., Soh, W., Song, S.R., 2006. Thermal history estimation of the Taiwan Chelungpu fault using rock-magnetic methods. Geophysical Research Letters 33, L23311.

Mishima, T., Hirono, T., Nakamura, N., Tanikawa, W., Soh, W., Song, S.R., 2009. Changes to magnetic minerals caused by frictional heating during the 1999 Taiwan Chi-Chi earthquake. Earth, Planets, and Space Letters 61, 797–801.

Moore, D., Lockner, D., 2004. Crystallographic controls on the frictional behavior of dry and water-saturated sheet structure minerals. Journal of Geophysical Research 109, B03401. http://dx.doi.org/10.1029/2003jb02582.

Niemeijer, A., Di Toro, G., Griffith, W.A., Bistacchi, A., Smith, S.A.F., Nielsen, S., 2012. Inferring earthquake physics and chemistry using an integrated field and laboratory approach. Journal of Structural Geology 39, 2–36. http://dx.doi.org/10.1016/j.jsg.2012.02.018.

Pec, M., Stünitz, H., Heilbronner, R., 2012. Semi-brittle deformation of granitoid gouges in shear experiments at elevated pressures and temperatures. Journal of Structural Geology 38, 200–221.

Pittarello, L.G., Di Toro, A., Bizzarri, G., Pennacchioni, J., Hadizadeh, M. Cocco, 2008. Energy partitioning during seismic slip in pseudotachylyte-bearing faults (Gole Larghe fault, Adamello, Italy). Earth and Planetary Science Letters 269, 131–139. http://dx.doi.org/10.1016/j.epsl.2008.01.052.

Reches, Z., Dewers, T.A., 2005. Gouge formation by dynamic pulverization during earthquake rupture. Earth and Planetary Science Letters 235, 361–374.

Rousset, B., Barbot, S., Avouac, J., Hsu, Y., 2012. Postseismic deformation following the 1999 Chi-Chi earthquake. Taiwan: Implication for lower-crust rheology. Journal of Geophysical Research 117. http://dx.doi.org/10.1029/2012JB009571.

Scholz, C.H., 2002. The Mechanics of Earthquakes and Faulting. Cambridge University Press, Cambridge, U.K. 158–167.

Sibson, R.H., 2003. Thickness of the seismic slip zone. Bulletin of the Seismological Society of America 93 (3), 1169–1178.

Tanaka, H., Wang, C.Y., Chen, W.M., Sakaguchi, A., Ujie, K., Ito, H., Ando, M., 2002. Initial science report of shallow drilling penetrating into the Chelungpu fault zone, Taiwan. Terrestrial Atmospheric and Oceanic Science 13, 227–251.

Tanaka, H., Chen, W.M., Kawabata, K., Urata, N., 2007. Thermal properties across the Chelungpu fault zone and evaluations of positive thermal anomaly on the slip zones: are these residuals of heat from faulting? Geophysical Research Letters 34, L01309. http://dx.doi.org/10.1029/2006GL028153.

Tinti, E., Spudich, P., Cocco, M., 2005. Earthquake fracture energy inferred from kinematic rupture models on extended faults. Journal of Geophysical Research 110 (B12), B12303.

Tomita, K., Yamane, H., Kawano, M., 1993. Synthesis of smectite from volcanic glass at low temperature. Clay and Clay Minerals 41 (6), 655–661.

Wilson, B., Dewers, T., Reches, Z., Brune, J., 2005. Particle size and energetics of gouge from earthquake rupture zone. Nature 434, 749–752.

Yue, L.F., Suppe, J., Hung, J.H., 2005. Structural geology of a classic thrust belt earthquake: the 1999 Chi-Chi earthquake Taiwan (Mw = 7.6). Journal of Structural Geology 27, 2058–2083.

Yund, R.A., Blanpied, M.L., Tullis, T.E., Weeks, J.D., 1990. Amorphous material in high strain experimental fault gouges. Journal of Geophysical Research 95 (B10), 15,589–15,602.

Zoback, M., Hickman, S., Ellsworth, W., 2010. Scientific drilling into the San Andreas fault zone: Eos. Transactions of the American Geophysical Union 91, 197–199. http://dx.doi.org/10.1029/2010EO220001.